

NACA RM L9E02



~~1111 2~~  
NACA  
64-112/100  
C.2

# RESEARCH MEMORANDUM

THE EFFECT OF SPAN AND DEFLECTION OF SPLIT  
FLAPS AND LEADING-EDGE ROUGHNESS ON THE LONGITUDINAL  
STABILITY AND GLIDING CHARACTERISTICS OF A 42°

SWEPTBACK WING EQUIPPED  
WITH LEADING-EDGE FLAPS

By

George L. Pratt and Thomas V. Bollech

Langley Aeronautical Laboratory  
Langley Air Force Base, Va.

**FOR REFERENCE**

**NOT TO BE TAKEN FROM THIS ROOM**

CLASSIFIED DOCUMENT

This document contains classified information affecting the National Defense of the United States within the meaning of the Espionage Act, USC 5021 and 5022. Its transmission or the revelation of its contents in any manner to an unauthorized person is prohibited by law. Information so classified may be imparted only to persons in the military and naval services of the United States, appropriate civilian officers and employees of the Federal Government who have a legitimate interest therein, and to United States citizens of known loyalty and discretion who of necessity must be informed thereof.

CLASSIFICATION CANCELLED

Authority: J. L. C. Crowley Date: 12/17/53  
J. E. D. 1.65-04  
By: [Signature] 12/17/53 see NACA  
A. E. [Signature] 1.638

## NATIONAL ADVISORY COMMITTEE FOR AERONAUTICS

WASHINGTON  
June 21, 1949

UNCLASSIFIED



UNCLASSIFIED

NATIONAL ADVISORY COMMITTEE FOR AERONAUTICS

RESEARCH MEMORANDUM

THE EFFECT OF SPAN AND DEFLECTION OF SPLIT  
FLAPS AND LEADING-EDGE ROUGHNESS ON THE LONGITUDINAL  
STABILITY AND GLIDING CHARACTERISTICS OF A 42°  
SWEEPBACK WING EQUIPPED  
WITH LEADING-EDGE FLAPS

By George L. Pratt and Thomas V. Bollech

## SUMMARY

The effect of half-span and full-span split flaps through a deflection range of 0° to 60° on the low-speed, longitudinal characteristics of a sweptback wing equipped with round-nose, extensible, leading-edge flaps was investigated at a Reynolds number of  $6.8 \times 10^6$ . Additional tests were made at a lower Reynolds number to determine the effect of leading-edge roughness on the longitudinal stability of the sweptback wing equipped with 0.725-semispan and 0.575-semispan leading-edge flaps. The wing had 42.05° sweep at the leading edge, an aspect ratio of 4.01, a taper ratio of 0.625, and NACA 641-112 airfoil sections perpendicular to the 0.273-chord line.

Although an increase in split-flap span increased the maximum lift, calculations of the power-off gliding characteristics indicate that the slight decrease in gliding speed obtainable with full-span flaps offers no appreciable advantages over half-span flaps. Both half-span and full-span split-flap deflections greater than 30° result in rapid increases in sinking speed with only a small reduction in gliding speed. For an assumed wing loading of 40 pounds per square foot, the full-span and half-span split flaps give sinking speeds in excess of 25 feet per second at all gliding speeds for flap deflections greater than 30° and 50°, respectively. The largest decrease in gliding speed for lowest increase in sinking speed is obtained by extending the leading-edge flaps with the trailing-edge flaps undeflected.

Neither half-span nor full-span split flaps had an appreciable effect on the stalling characteristics of the wing equipped with leading-edge flaps in the range of split-flap deflections tested.

~~RESTRICTED~~

UNCLASSIFIED

Leading-edge roughness caused an undesirable variation of pitching moment at maximum lift when applied to the wing with 0.725-semispan leading-edge flaps but had little effect on the longitudinal stability with 0.575-semispan leading-edge flaps.

### INTRODUCTION

In an attempt to improve the low-speed longitudinal characteristics of sweptback wings, various combinations of high-lift and stall-control devices have been tested in the Langley 19-foot pressure tunnel on a 42° sweptback wing having NACA 64<sub>1</sub>-112 airfoil sections. The results of these tests are reported in references 1 and 2.

In order to supplement these tests, the present investigation has been conducted primarily to determine the effect of full-span and half-span split flaps on the 42° sweptback wing through a flap-deflection range of 60°. It is expected that sweptback-wing airplanes will require some leading-edge device to eliminate the inherent longitudinal instability usually associated with swept wings at stalling angles of attack. The split flaps have been tested, therefore, in conjunction with a 0.575-semispan, round-nose, extensible, leading-edge flap which has been shown to provide stability at the stall with and without split flaps (reference 2). An analysis has been made to determine the effect of split-flap span and deflection on the power-off gliding characteristics of the 42° sweptback wing operating with an assumed wing loading condition.

Roughness in the form of carborundum granules was applied to the leading edge of the wing to determine the effect of surface condition on the stability of a sweptback wing with a leading-edge flap deflected.

The split-flap tests were made at a Reynolds number of  $6.8 \times 10^6$  and a Mach number of approximately 0.16. The effect of roughness was determined at Reynolds numbers of  $3.0 \times 10^6$  and  $4.7 \times 10^6$ .

### SYMBOLS

The data are presented in standard NACA coefficient and symbol notation. The forces and moments are measured about a system of wind axes with the origin located on the root of the wing at a point corresponding to the quarter-chord point of the mean aerodynamic chord.

$C_L$  lift coefficient  $\left( \frac{\text{Lift}}{qS} \right)$

$C_{L_{trim}}$	lift coefficient corrected for tail lift required to trim the pitching moment to zero (tail length equals $3\bar{c}$ and $\frac{q_t}{q}$ assumed equal to 1.0) $\left(C_L + \frac{C_m}{3}\right)$
$C_D$	drag coefficient $\left(\frac{\text{Drag}}{qS}\right)$
L/D	lift-drag ratio
$C_m$	pitching-moment coefficient about $0.25\bar{c}$ $\left(\frac{\text{Pitching moment}}{qS\bar{c}}\right)$
$\alpha$	angle of attack, degrees
V	free-stream velocity, feet per second
$\rho$	mass density of air, slugs per cubic foot
q	free-stream dynamic pressure, pounds per square foot $\left(\frac{1}{2}\rho V^2\right)$
$q_t$	free-stream dynamic pressure at the assumed tail position, pounds per square foot
S	basic wing area, square feet
c	local wing chord parallel to plane of symmetry, feet
$\bar{c}$	mean aerodynamic chord parallel to plane of symmetry, feet $\left(\frac{2}{b} \int_0^{b/2} c^2 dy\right)$
b	wing span, feet
y	spanwise coordinate
$\delta_f$	split-flap deflection, degrees
$\theta$	angle of glide, degrees $\left(\cot^{-1} \frac{L}{D}\right)$
$V_G$	gliding speed, miles per hour
$V_S$	stalling speed, miles per hour
$V_V$	sinking speed, feet per second
R	Reynolds number $\left(\frac{\rho V \bar{c}}{\mu}\right)$

$\mu$  coefficient of viscosity

$\bar{x}$  distance from leading edge of root section to origin of axes system

Subscript:

max maximum

#### MODEL

The model was constructed of laminated mahogany to conform to the plan form and dimensions given in figure 1. The wing had an aspect ratio of 4.01, a taper ratio of 0.625, an angle of sweepback of  $42.05^\circ$  at the leading edge, and NACA 64<sub>1</sub>-112 airfoil sections perpendicular to the 0.273-chord line. The 0.273-chord line corresponds to the quarter-chord line of the wing before the wing panels were swept back. The wing had no geometric twist or dihedral.

The split flaps (fig. 2(a)) were constructed of sheet steel and were attached to the wing with wooden brackets. Flap deflections of  $15^\circ$ ,  $30^\circ$ ,  $45^\circ$ , and  $60^\circ$  with the lower wing surface measured perpendicular to the 0.273-chord line were obtained by varying the angle of the attachment brackets. The chord of the flap was equal to 18.4 percent of the local wing chord in the stream direction or 20 percent of the chord measured perpendicular to the 0.273-chord line. The half-span and full-span flaps extended from the plane of symmetry to  $0.5\frac{b}{2}$  and  $0.975\frac{b}{2}$ , respectively.

The round-nose, extensible, leading-edge flaps (fig. 2(b)) were of constant chord and extended from  $0.4\frac{b}{2}$  to  $0.975\frac{b}{2}$  and from  $0.25\frac{b}{2}$  to  $0.975\frac{b}{2}$  for the  $0.575\frac{b}{2}$  and  $0.725\frac{b}{2}$  flaps, respectively. The flap chord was approximately 14.3 percent of the wing chord perpendicular to the 0.273-chord line at the outboard end and 10 percent at the inboard end ( $0.25\frac{b}{2}$ ).

Prior to the present investigation, the wing had been altered for the addition of a leading-edge slat and the data of the plain wing with the slat retracted, which have been presented for comparative purposes (fig. 3), do not give the same lift characteristics at high angles of attack of the unaltered wing as reported in reference 3. There was little effect, however, on the aerodynamic characteristics of the wing when a leading-edge flap was added to the portion of the wing fitted with the slat.

Leading-edge roughness was obtained by applying No. 60 carborundum grains to a thin coating of shellac on approximately 2 inches of the upper and lower surfaces of the portion of the wing not fitted with the leading-edge flap measured along the surface of the wing from the leading edge. Roughness was also applied to the initial 2 inches of the upper surface of the leading-edge flap.

Figure 4 shows the model equipped with the  $0.575\frac{b}{2}$  leading-edge flaps and half-span split flaps.

### TESTS

The model was mounted on the two-support system of the Langley 19-foot pressure tunnel as shown in figure 4. The tests were made with the air in the tunnel compressed to approximately  $2\frac{1}{3}$  atmospheres. The split-flap tests were made at a Reynolds number of  $6.8 \times 10^6$ , and the effect of leading-edge roughness on the wing equipped with leading-edge flaps was determined at Reynolds numbers of  $3.0 \times 10^6$  and  $4.7 \times 10^6$ . Lift, drag, and pitching-moment characteristics were obtained through an angle-of-attack range from  $-4^\circ$  through the stall. The stalling characteristics were determined by observation of wool tufts attached to the upper surface of the wing.

The lift, drag, and pitching-moment data have been corrected for support tare and interference effects. Air-stream misalignment corrections have been applied to the angle-of-attack and drag coefficients.

The angle of attack and drag have also been corrected for jet-boundary effects and the pitching moment corrected for tunnel-induced distortion of the loading using the corrections presented in reference 3.

### RESULTS AND DISCUSSION

In order to provide a basic model configuration which would result in a stable break in the pitching moment at the stall, a  $0.575\frac{b}{2}$  leading-edge flap was installed on the outboard portion of the wing throughout the split-flap investigation. It has been shown that, in addition to its stabilizing effect, the  $0.575\frac{b}{2}$  leading-edge flap produced an increment of  $C_{l_{max}}$  of 0.22 over that obtained for the plain wing (figs. 3 and 5).

Effect of split-flap deflection on lift and stalling characteristics.-

The effect of varying the deflection of half-span and full-span split flaps on the lift and stalling characteristics of the  $42^\circ$  sweptback wing are presented in figures 5 to 7. A cross plot of maximum lift versus flap deflection (fig. 6) indicates that in proportion to their respective spans and at moderate deflections, the full-span split flaps were more effective in increasing maximum lift coefficient than the half-span split flaps. At a deflection of  $60^\circ$  the increase in lift coefficient was proportional to the flap span and resulted in increments of  $C_{L_{max}}$  of 0.16 and 0.32 for the half-span and full-span flaps, respectively.

In the range of split-flap deflections tested neither the half-span nor full-span flaps had an appreciable effect on the longitudinal stability of the wing equipped with leading-edge flaps. The half-span flaps deflected  $30^\circ$  (fig. 5) resulted in a slight tendency toward instability before the stall, but the pitching moment broke in a stable direction at the stall.

It should be pointed out that the wing was equipped with an aileron which deflected slightly during the flap tests. This deflection resulted in a slight forward movement of the wing center of pressure when compared with data from previous tests. (The effect was eliminated during the roughness tests by attaching the aileron rigidly to the wing.) The pitching-moment variation for the two aileron conditions is shown in figure 5. Similar changes would occur for the split-flap-deflected configurations.

Observation of wool tufts on the upper surface of the wing indicate that half-span and full-span split flaps had little effect on the manner in which the stalling pattern spread over the surface of the wing with increasing angle of attack (fig. 7).

Effect of split flaps on gliding characteristics.- The power-off gliding characteristics of the  $42^\circ$  sweptback wing with  $0.575\frac{1}{2}$  leading-edge flaps and half-span and full-span split flaps at various deflections are presented in figure 8. Contours of constant values of gliding speed and sinking speed for an airplane having a wing loading of 40 pounds per square foot have been superimposed on the curves of lift-drag ratio versus lift coefficient for the various configurations. The gliding angles corresponding to the values of lift-drag ratio are also presented. The experimental lift-coefficient values have been corrected for the tail lift required to trim the pitching moment (fig. 5) to zero for an assumed value of  $q_t/q$  of 1.0 through the lift range and tail length equal to  $3\bar{c}$ . No attempt has been made to correct for the effects of fuselage, nacelles, landing gear, and other protuberances associated with an actual airplane, and the following discussion is based on the power-off condition only.

In order to show more clearly the effects of split-flap span and deflection on the gliding characteristics, a cross plot of sinking speed versus gliding speed for various deflections and spans is presented in figure 9. Data for the wing without leading-edge or trailing-edge flaps are also presented for comparison. Values corresponding to a gliding speed 20 percent above stalling speed have been indicated on this figure for the various configurations. The  $1.2V_s$  point is believed to be the minimum excess speed that would be used in a landing approach.

Based on an arbitrary maximum desired rate of descent of 25 feet per second and the assumed loading conditions, the half-span split flap deflected  $60^\circ$  would result in undesirable sinking speeds at all gliding velocities. The half-span split flap deflected  $45^\circ$  would provide desirable sinking speeds within a small range of gliding speeds, while deflections of  $30^\circ$  or less would give desirable sinking speeds at all gliding speeds which may be expected in a landing approach. Full-span split-flap deflections greater than  $30^\circ$  result in sinking speeds greater than the desired maximum at all gliding velocities.

A comparison of full-span and half-span split flaps at the same deflection (fig. 9) indicates that, although the full-span split flaps give a decrease in gliding speed, this advantage is largely offset by the increased rate of descent. From a comparison of the full-span and half-span flaps at a given sinking speed, it appears that the slight decrease in gliding speed and lower deflection required for the full-span flap offer no appreciable advantages over the half-span flap. It is interesting to note that the greatest decrease in gliding speed for lowest increase in sinking speed is obtained by deflecting the leading-edge flaps alone.

Effect of leading-edge roughness on longitudinal stability.- Low-scale tests of a semispan model of the same plan form and profile in the Langley two-dimensional low-turbulence pressure tunnel (reference 4) have shown that surface condition may have an appreciable effect on the stability of sweptback wings fitted with leading-edge flaps. The model with  $0.725\frac{b}{2}$  leading-edge flaps and half-span split flaps was found to be stable at the stall when in a smooth condition at Reynolds numbers of  $5.2 \times 10^6$  and  $6.8 \times 10^6$  but unstable at a Reynolds number of  $3.0 \times 10^6$ . (This unstable break at a Reynolds number of  $3.0 \times 10^6$  has been attributed to boundary-layer effects of the tunnel wall at the root of the semispan model.) The application of roughness to the leading edge, however, resulted in an unstable break in the pitching moment at all three Reynolds numbers.

Tests of a similar configuration on the full-span model in the Langley 19-foot pressure tunnel at a Reynolds number of  $3.0 \times 10^6$

(fig. 10) show that the pitching-moment curve broke in a stable direction for the smooth wing but varied in an erratic and undesirable manner at the stall when roughness was applied to the leading edge.

Leading-edge roughness had little effect on the stability of the wing fitted with  $0.575\frac{b}{2}$  leading-edge flaps with and without half-span split flaps (fig. 11).

The effect of leading-edge roughness on the air flow on the upper surface of the wing is indicated in figures 12 and 13. Tip stalling at high angles of attack resulted in the undesirable pitching-moment characteristics of the  $0.725\frac{b}{2}$  leading-edge-flap configuration with roughness. It appears that in the selection of a leading-edge-flap span to provide a longitudinal stabilizing effect at the stall, consideration should be given to surface conditions which may influence the stability of the wing for certain critical flap spans.

#### CONCLUSIONS

The following conclusions may be made from the tests of the  $42^\circ$  sweptback wing with various split-flap deflections and spans and the tests of the leading-edge flaps with roughness:

1. Although an increase in split-flap span increased the maximum lift, calculations of the power-off gliding characteristics indicate that the slight decrease in gliding speed obtainable with a full-span flap offers no appreciable advantages over half-span flaps. Both half-span and full-span split-flap deflections greater than  $30^\circ$  result in rapid increases in sinking speed with only a small reduction in gliding speed. For an assumed wing loading of 40 pounds per square foot, the full-span and half-span split flaps give sinking speeds in excess of 25 feet per second at all gliding speeds for flap deflections greater than  $30^\circ$  and  $50^\circ$ , respectively. The largest decrease in gliding speed for lowest increase in sinking speed is obtained by extending the leading-edge flaps with the trailing-edge flaps undeflected.

2. Neither half-span nor full-span split flaps had an appreciable effect on the stalling characteristics of the wing equipped with leading-edge flaps in the range of split-flap deflections tested.

3. Leading-edge roughness caused an undesirable variation of pitching moment at maximum lift when applied to the wing with 0.725-semispan leading-edge flaps but had little effect on the longitudinal stability with 0.575-semispan leading-edge flaps.

Langley Aeronautical Laboratory  
National Advisory Committee for Aeronautics  
Langley Air Force Base, Va.

#### REFERENCES

1. Conner, D. William, and Neely, Robert H.: Effects of a Fuselage and Various High-Lift and Stall-Control Flaps on Aerodynamic Characteristics in Pitch of an NACA 64-Series  $40^\circ$  Swept-Back Wing. NACA RM L6I27, 1947.
2. Graham, Robert R., and Conner, D. William: Investigation of High-Lift and Stall-Control Devices on an NACA 64-Series  $42^\circ$  Sweptback Wing with and without Fuselage. NACA RM L7G09, 1947.
3. Neely, Robert H., and Conner, D. William: Aerodynamic Characteristics of a  $42^\circ$  Swept-Back Wing with Aspect Ratio 4 and NACA 64<sub>1</sub>-112 Airfoil Sections at Reynolds Numbers from 1,700,000 to 9,500,000. NACA RM L7D14, 1947.
4. Cahill, Jones F.: Comparison of Semispan Data Obtained in the Langley Two-Dimensional Low-Turbulence Pressure Tunnel and Full-Span Data Obtained in the Langley 19-Foot Pressure Tunnel for a Wing with  $40^\circ$  Sweepback of the 0.27-Chord Line. NACA RM L9B25a, 1949.

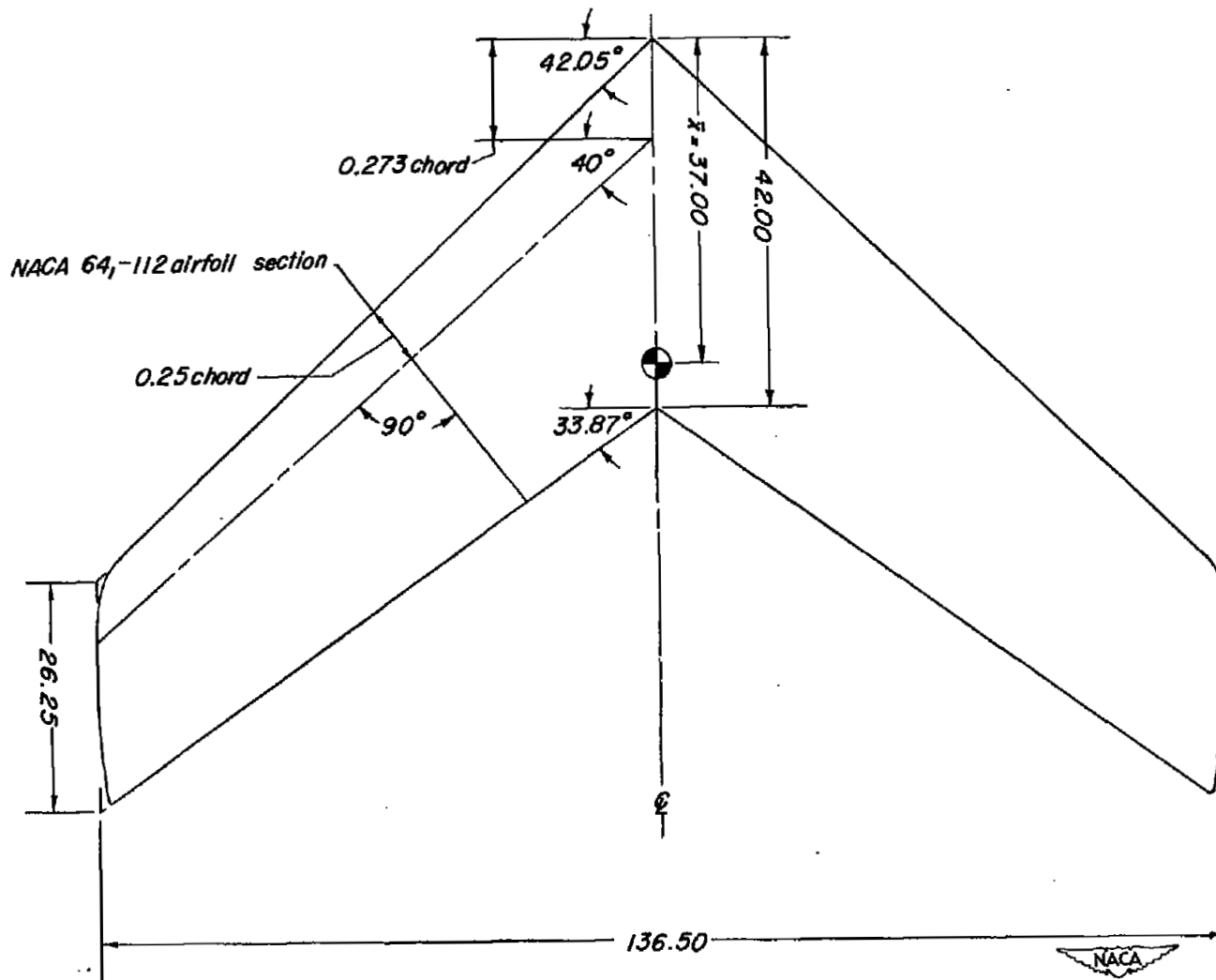
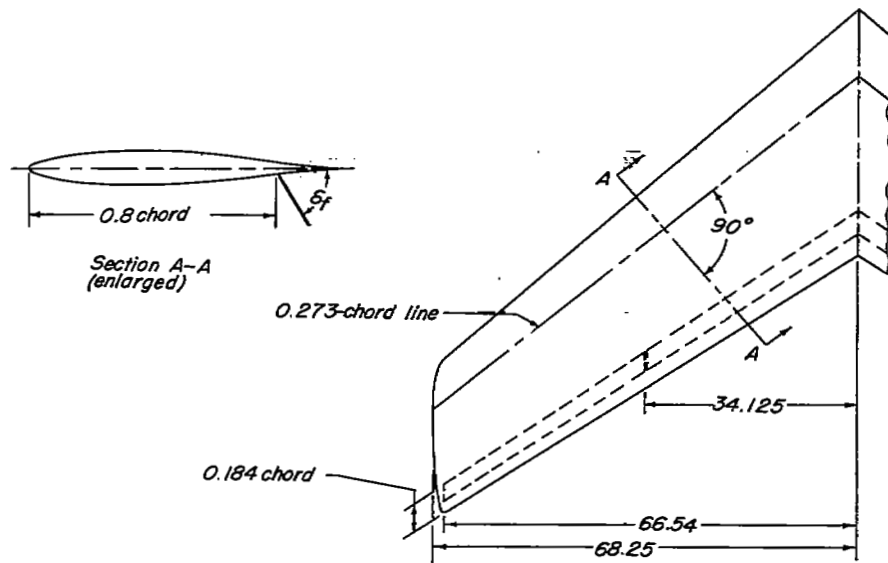
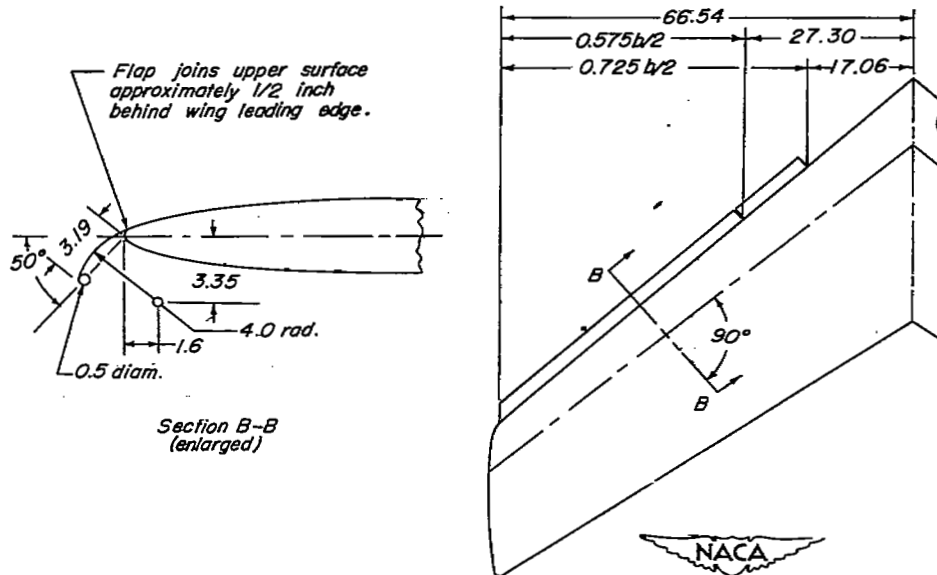


Figure 1.- Plan form of 42° sweptback wing. Area, 32.24 square feet; mean aerodynamic chord, 2.892 feet; aspect ratio, 4.01; taper ratio, 0.625. (All dimensions in inches.)



(a) Split flaps.



(b) Leading-edge flaps.

Figure 2.- Details of trailing-edge split flaps and round-nose, extensible, leading-edge flap. (All dimensions are in inches.)

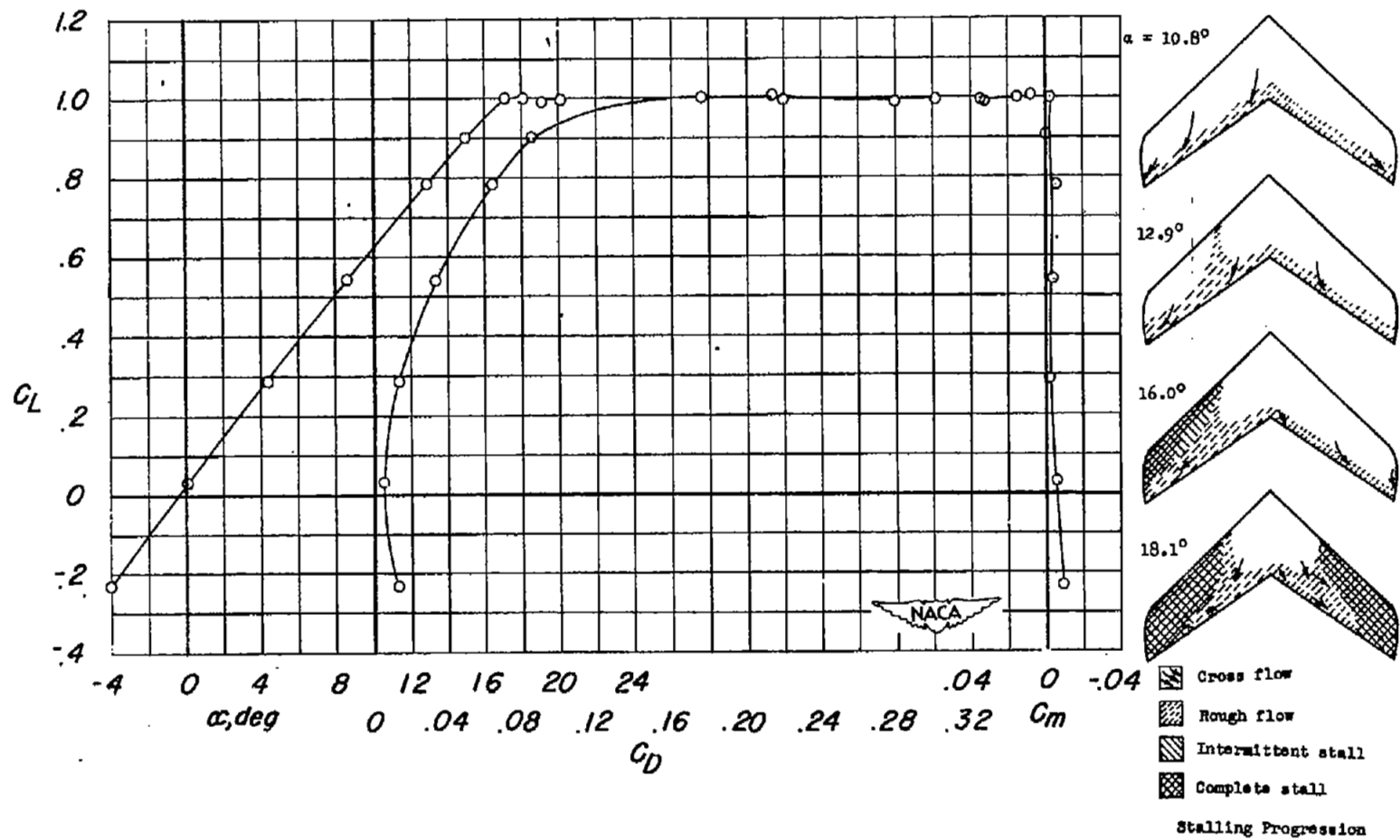


Figure 3.- Aerodynamic characteristics of a 42° sweptback wing.  $R = 6.8 \times 10^6$ .

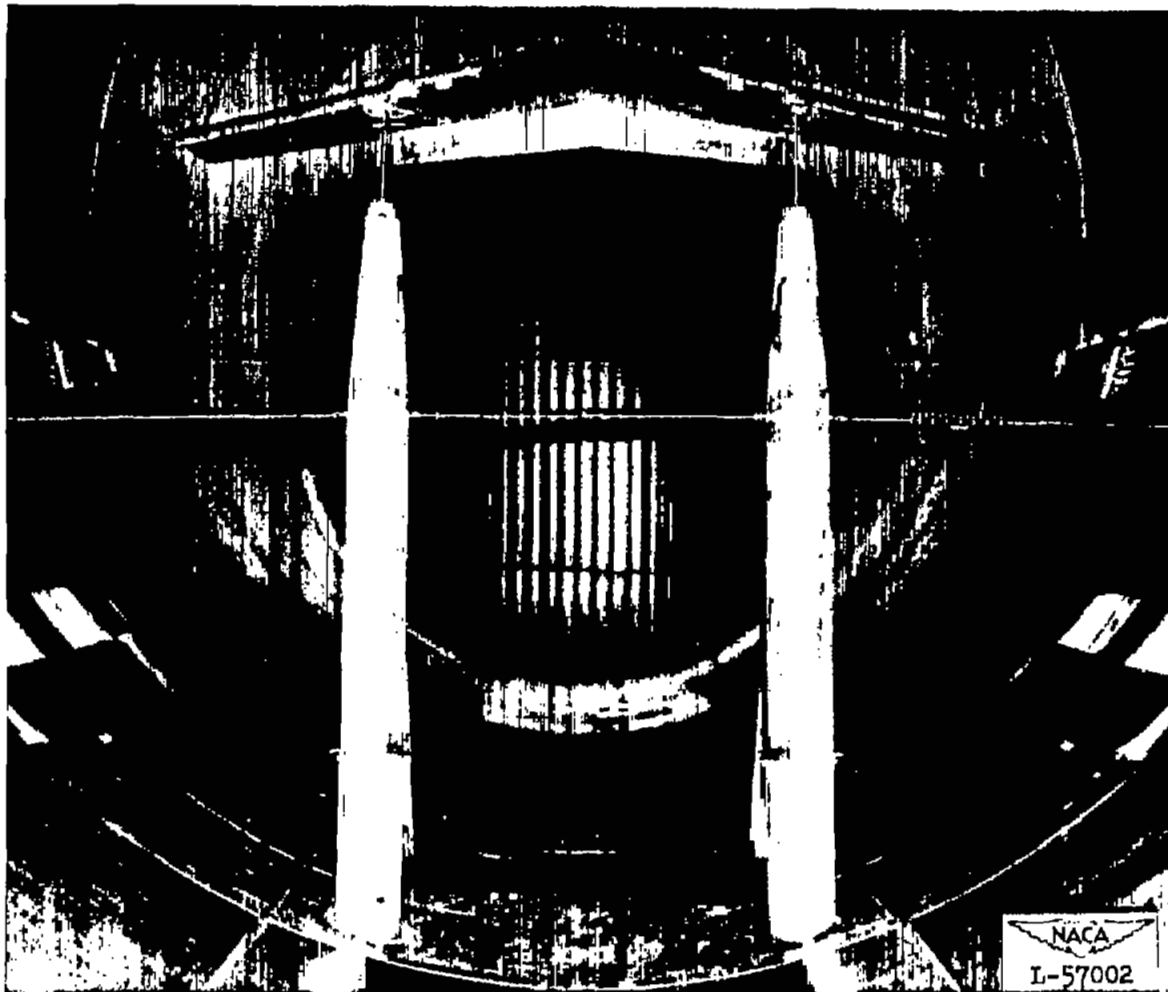
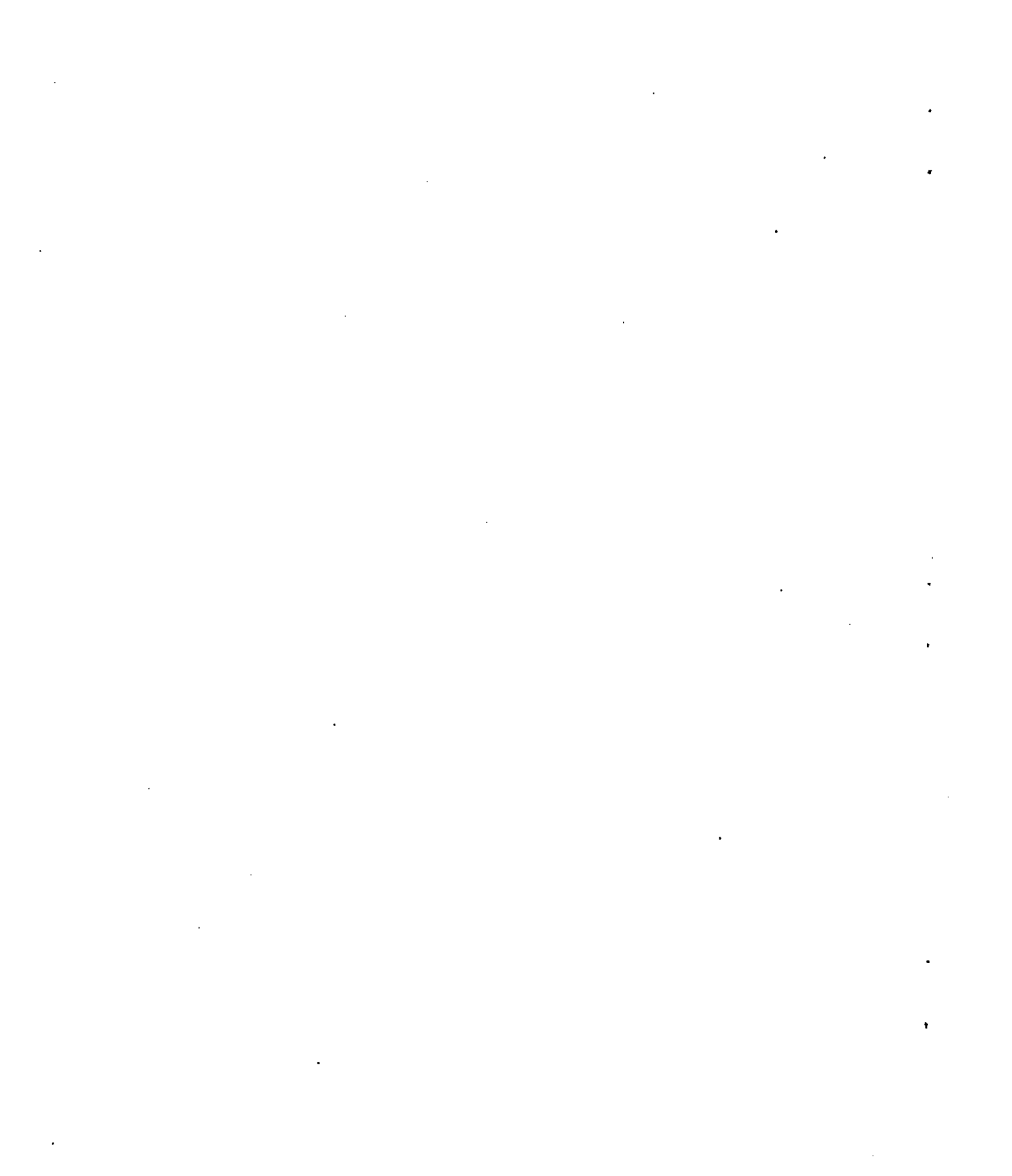
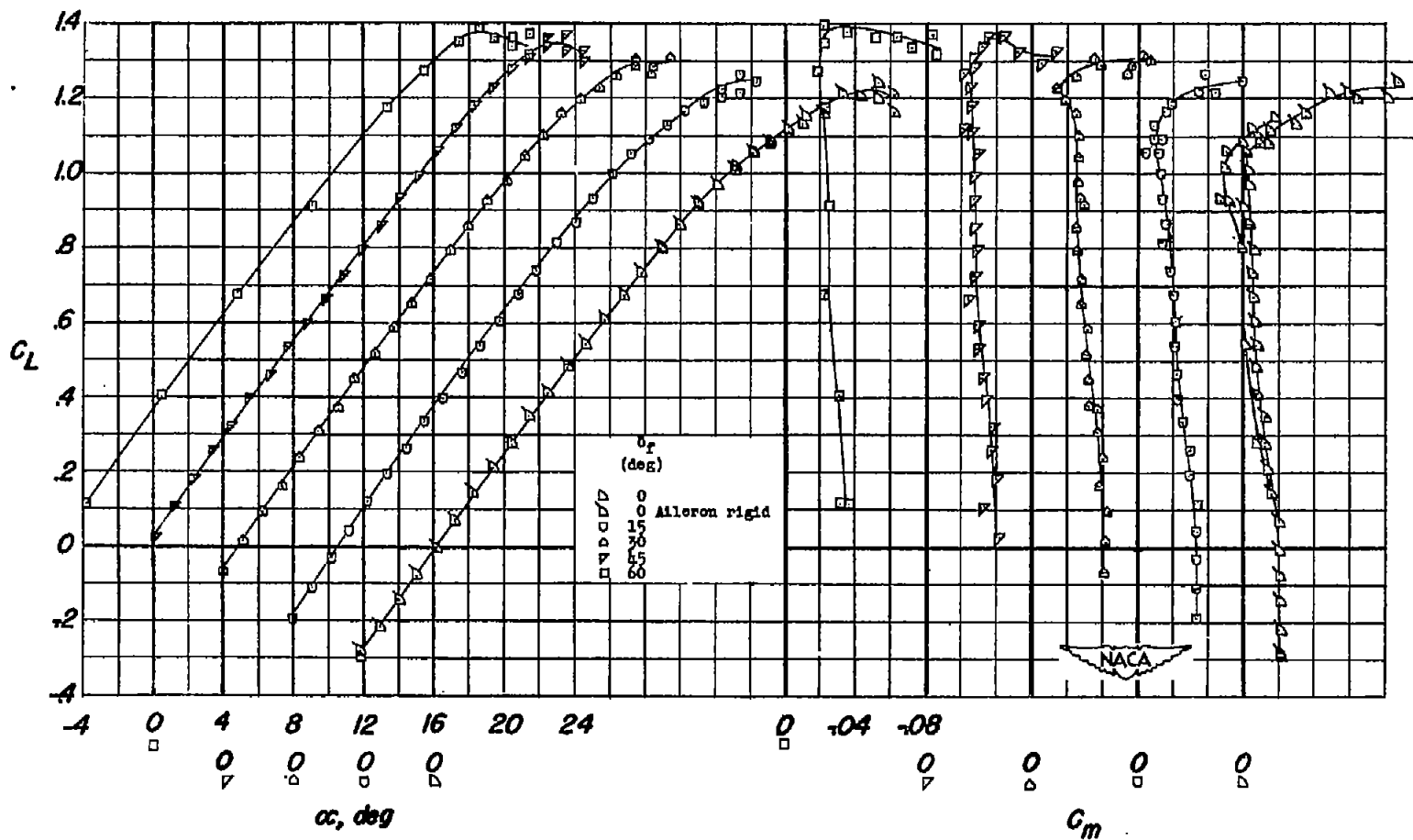


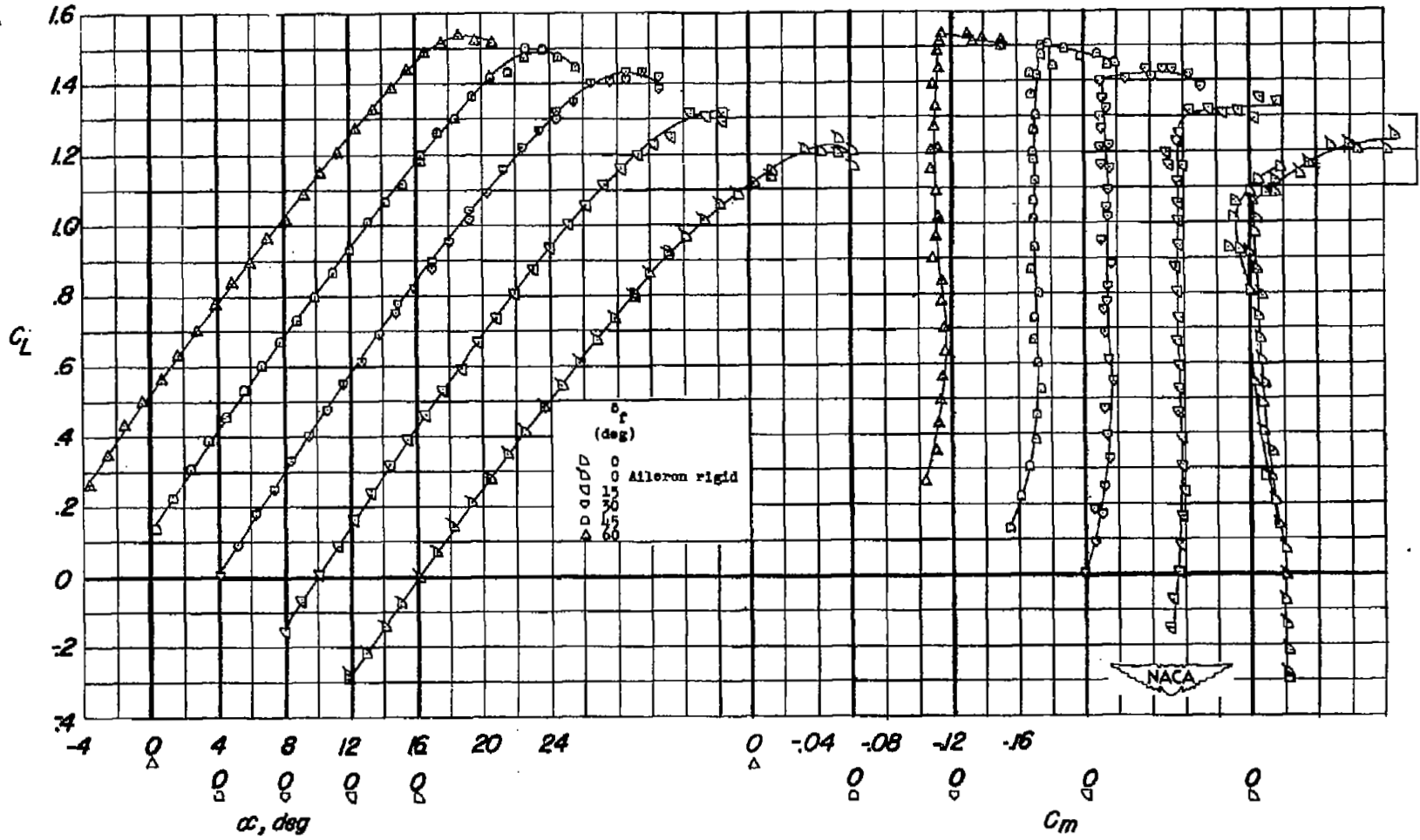
Figure 4.- The  $42^\circ$  sweptback wing mounted for test with  $0.575\frac{b}{2}$  leading-edge flaps and half-span split flaps.





(a) Half-span split flaps.

Figure 5.- Aerodynamic characteristics of a  $42^\circ$  sweptback wing with  $0.575\frac{b}{2}$  leading-edge flaps at various split-flap deflections.  $R = 6.8 \times 10^6$ .



(b) Full-span split flaps.

Figure 5.- Concluded.

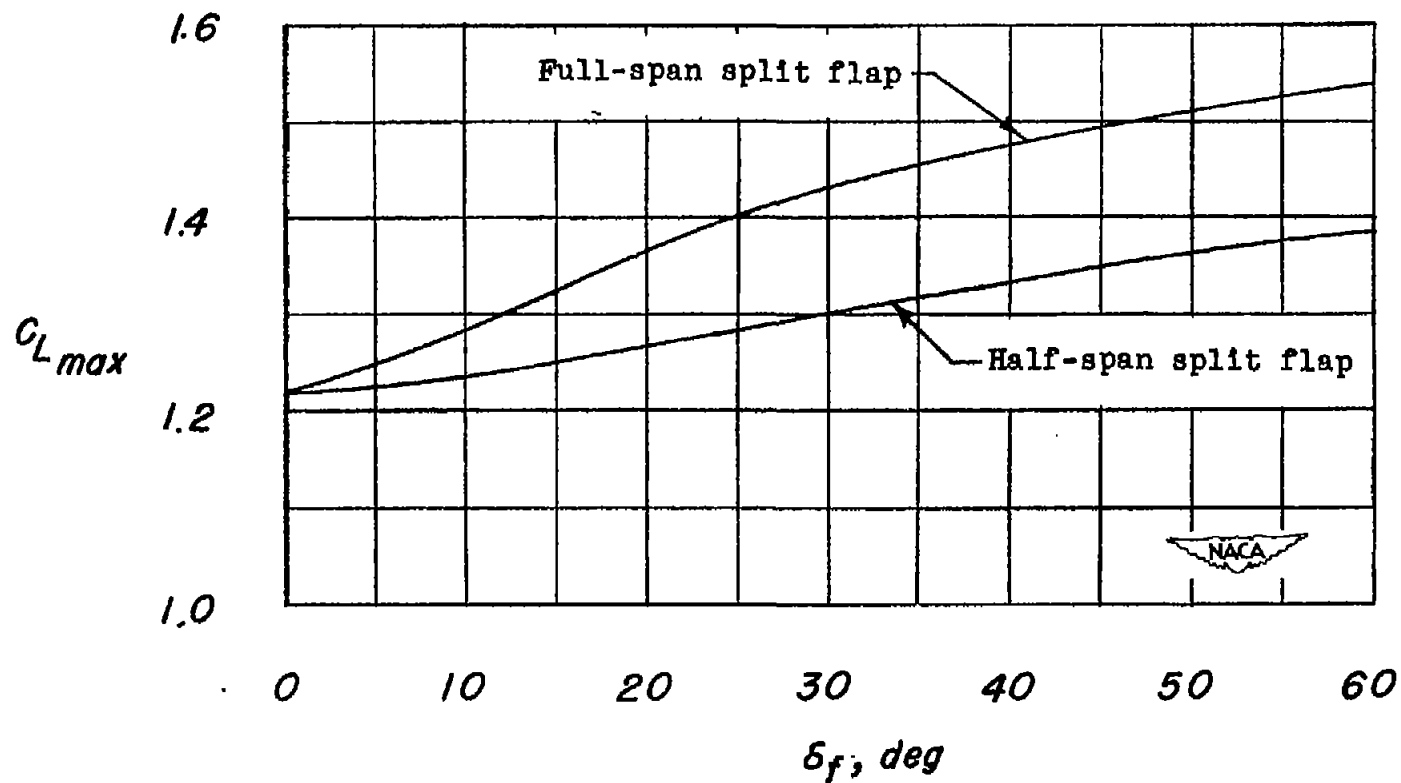
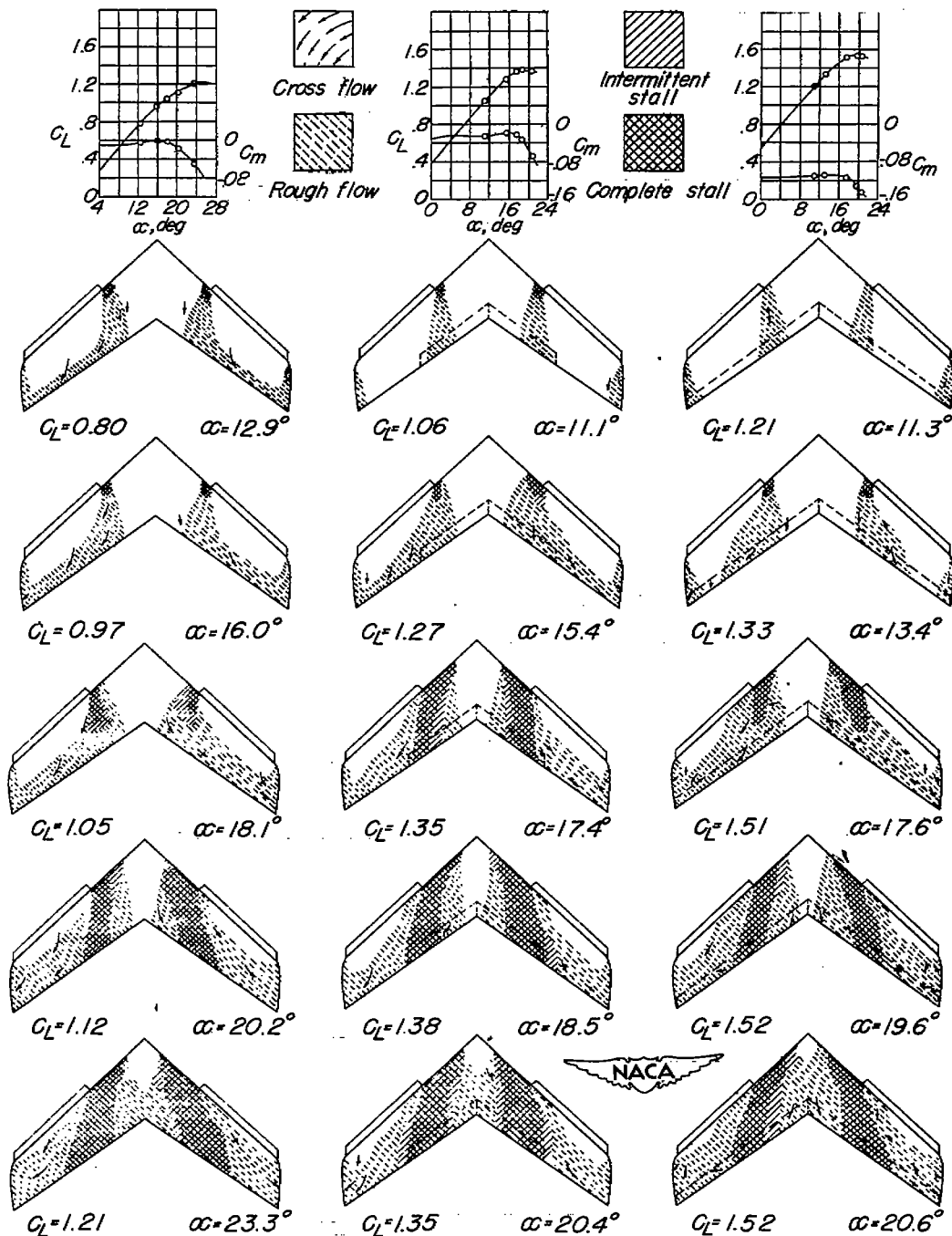


Figure 6.- Variation of  $C_{L_{max}}$  with split-flap deflection on a  $42^\circ$  sweptback wing with  $0.575\frac{b}{2}$  leading-edge flaps.  $R = 6.8 \times 10^6$ .



(a) Split flaps off. (b) Half-span split flaps. (c) Full-span split flaps.

Figure 7.- Stalling characteristics of the 42° sweptback wing with 0.575  $\frac{b}{2}$  leading-edge flaps and trailing-edge split flaps.  $\delta_f = 60^\circ$ ;  $R = 6.8 \times 10^6$ .

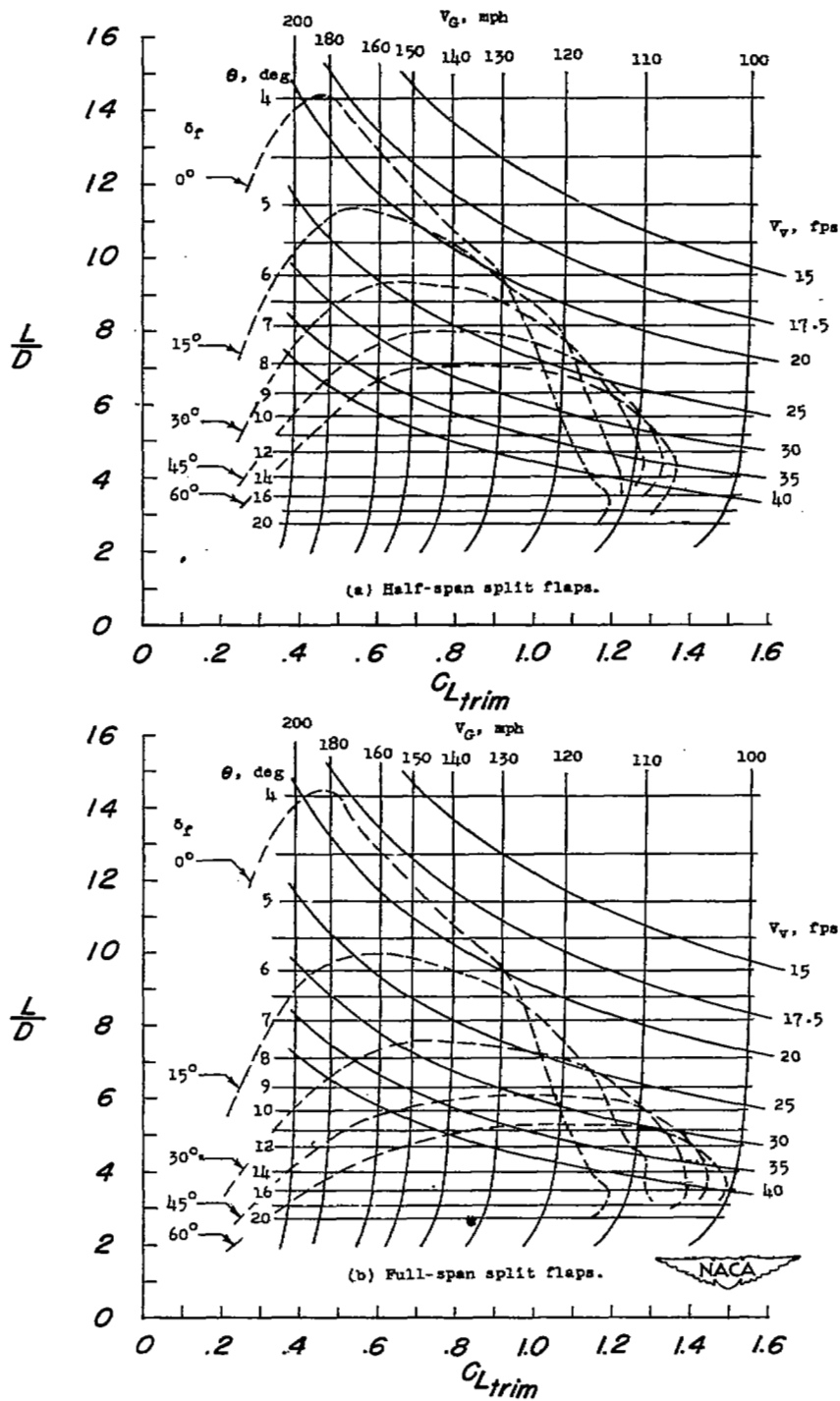
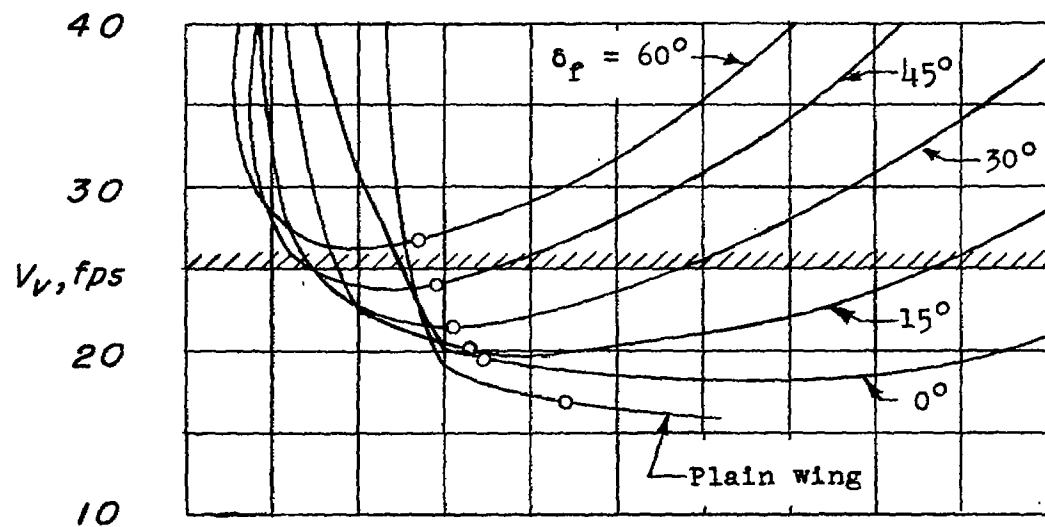
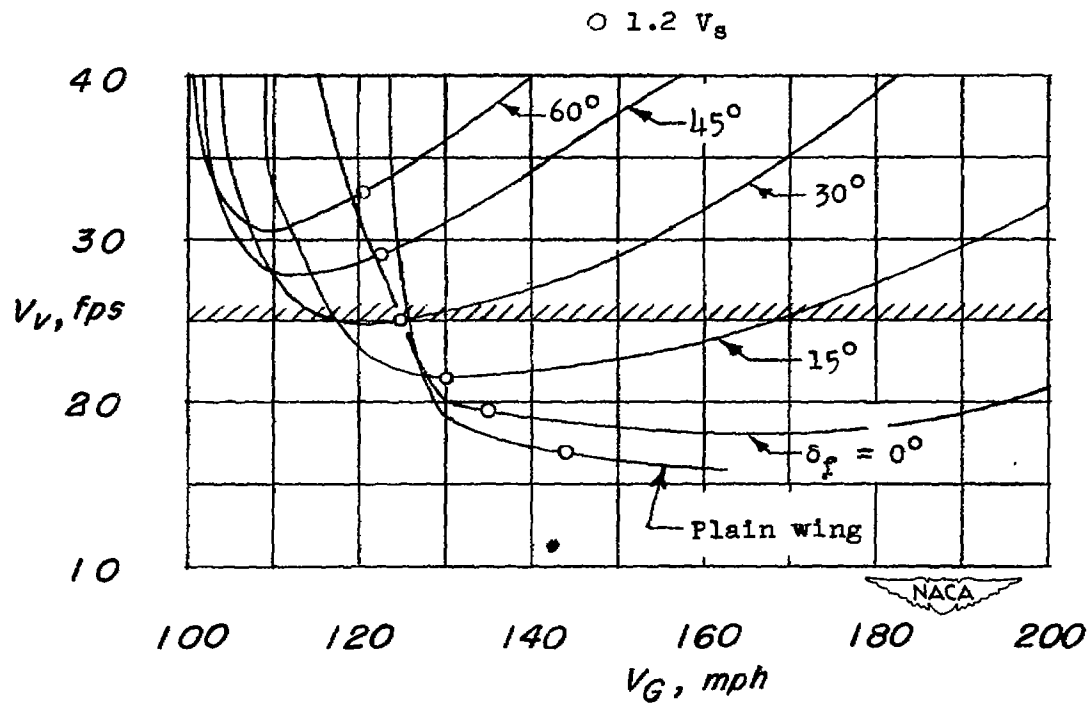


Figure 8.- Glide characteristics of a  $42^\circ$  sweptback wing with  $0.575\frac{b}{2}$  leading-edge flaps at various split-flap deflections. Wing loading, 40 pounds per square foot;  $R = 6.8 \times 10^6$ .



(a) Half-span split flap.



(b) Full-span split flap.

Figure 9.- Effect of split flaps on the gliding characteristics of the  $42^\circ$  sweptback wing.

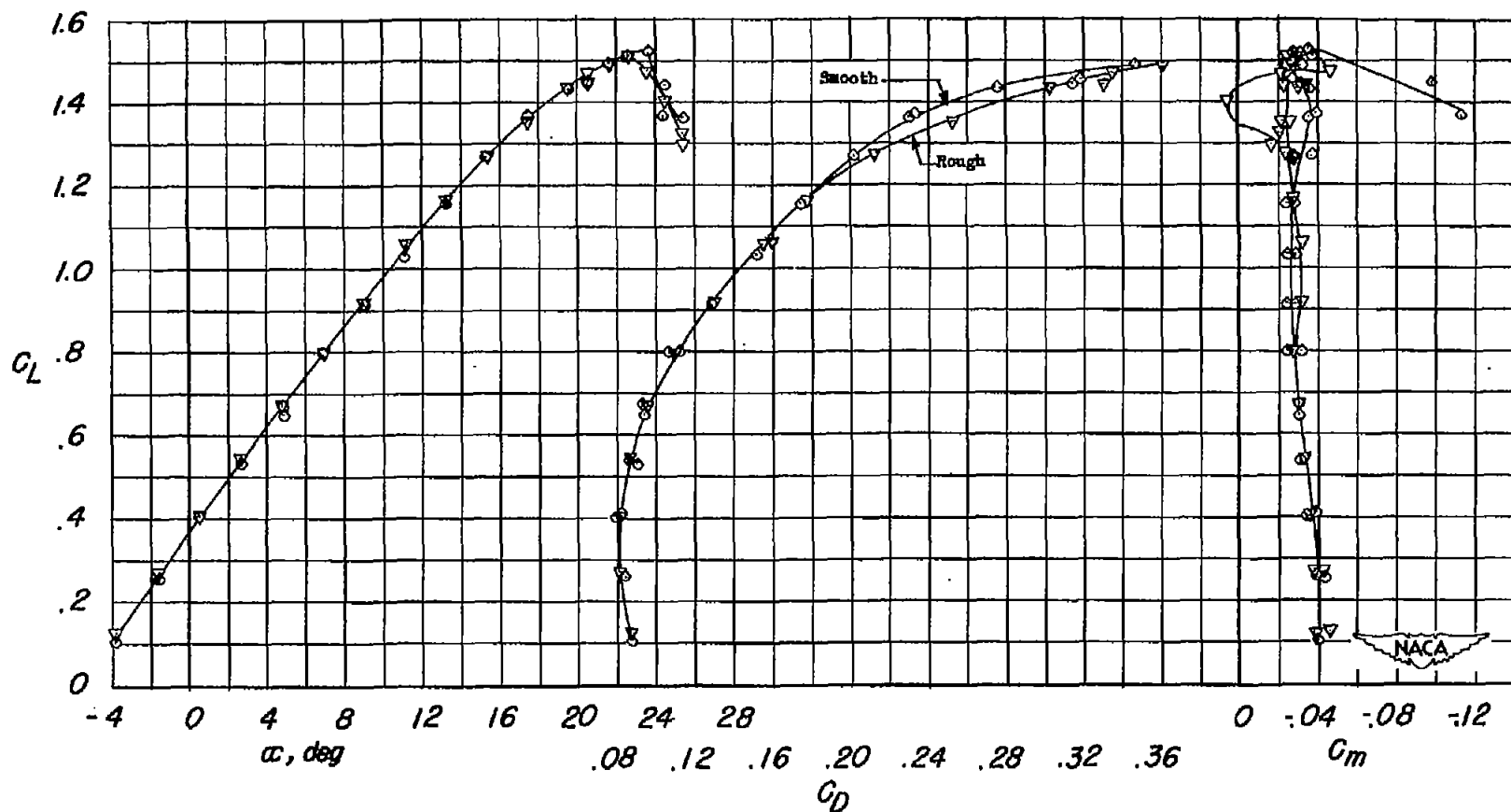
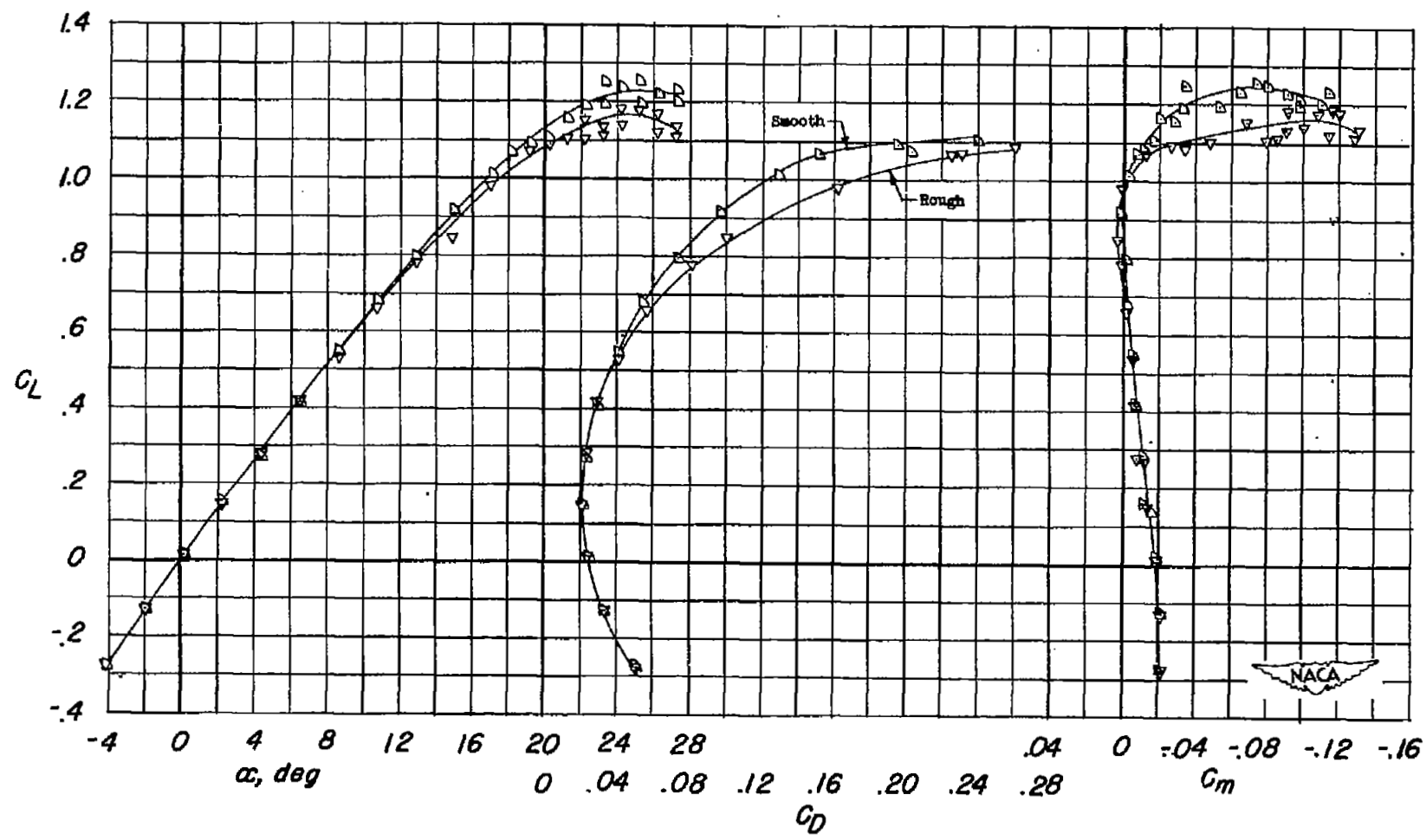
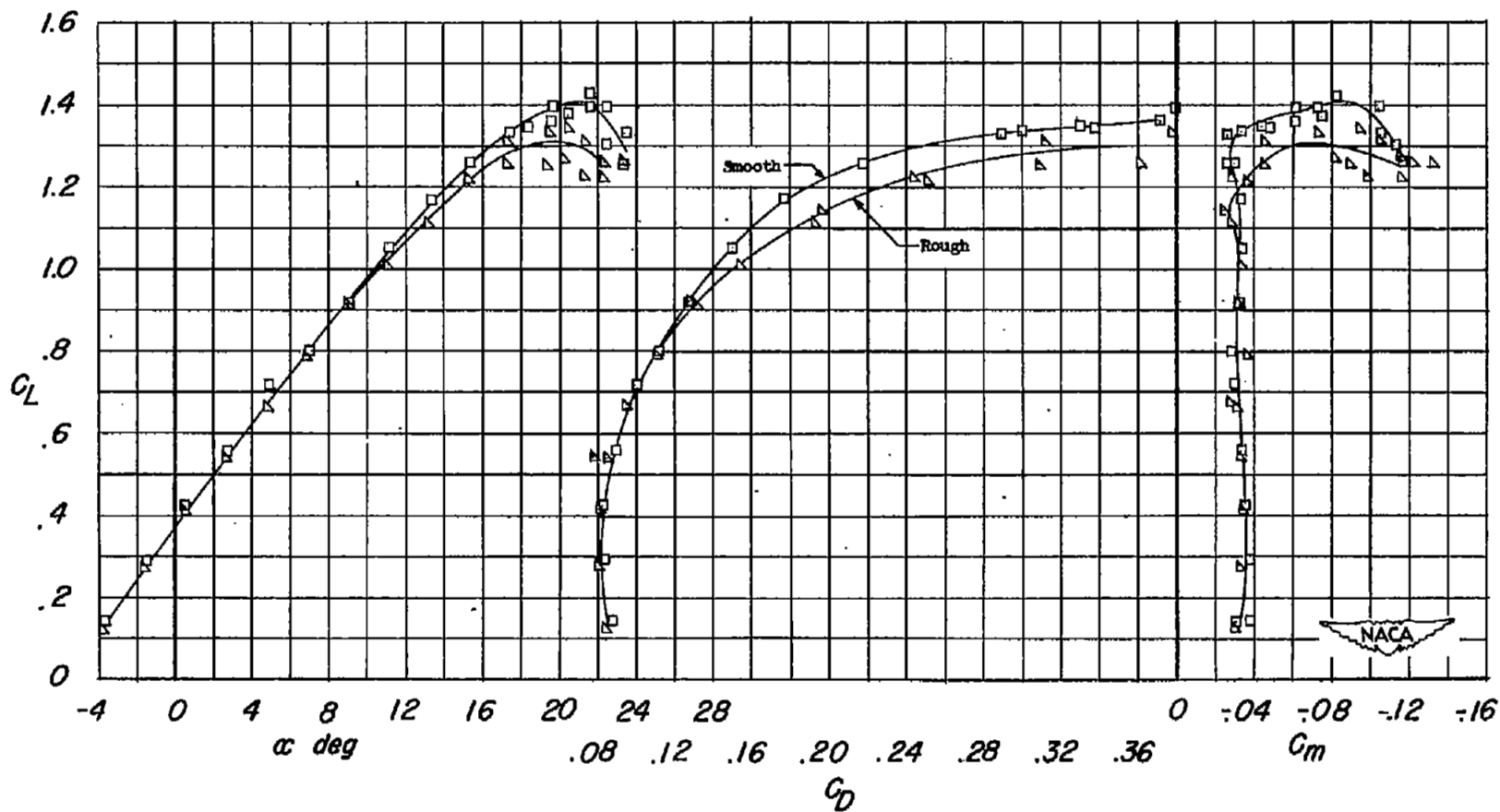


Figure 10.- Aerodynamic characteristics of a  $42^\circ$  sweptback wing with  $0.725\frac{b}{2}$  leading-edge flaps and half-span split flaps with and without leading-edge roughness.  $R = 3.0 \times 10^6$ ;  $\delta_f = 60^\circ$ .



(a) Split flaps off;  $\delta_f = 60^\circ$ ;  $R = 4.7 \times 10^6$ .

Figure 11.- Aerodynamic characteristics of a  $42^\circ$  sweptback wing with  $0.575\frac{b}{2}$  leading-edge flaps with and without leading-edge roughness.



(b) Half-span split flaps on;  $\delta_f = 60^\circ$ ;  $R = 3.0 \times 10^6$ .

Figure 11.- Concluded.

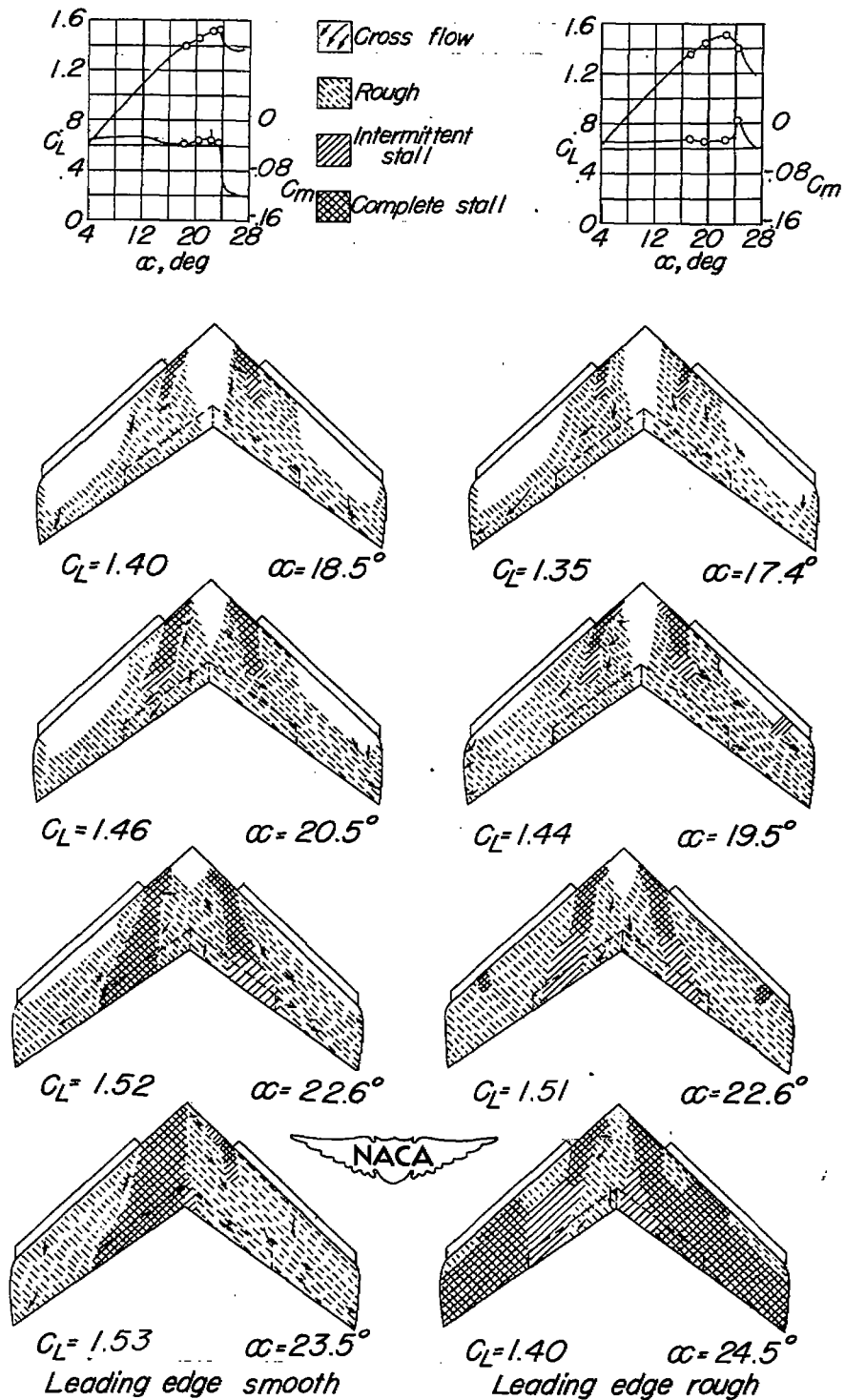
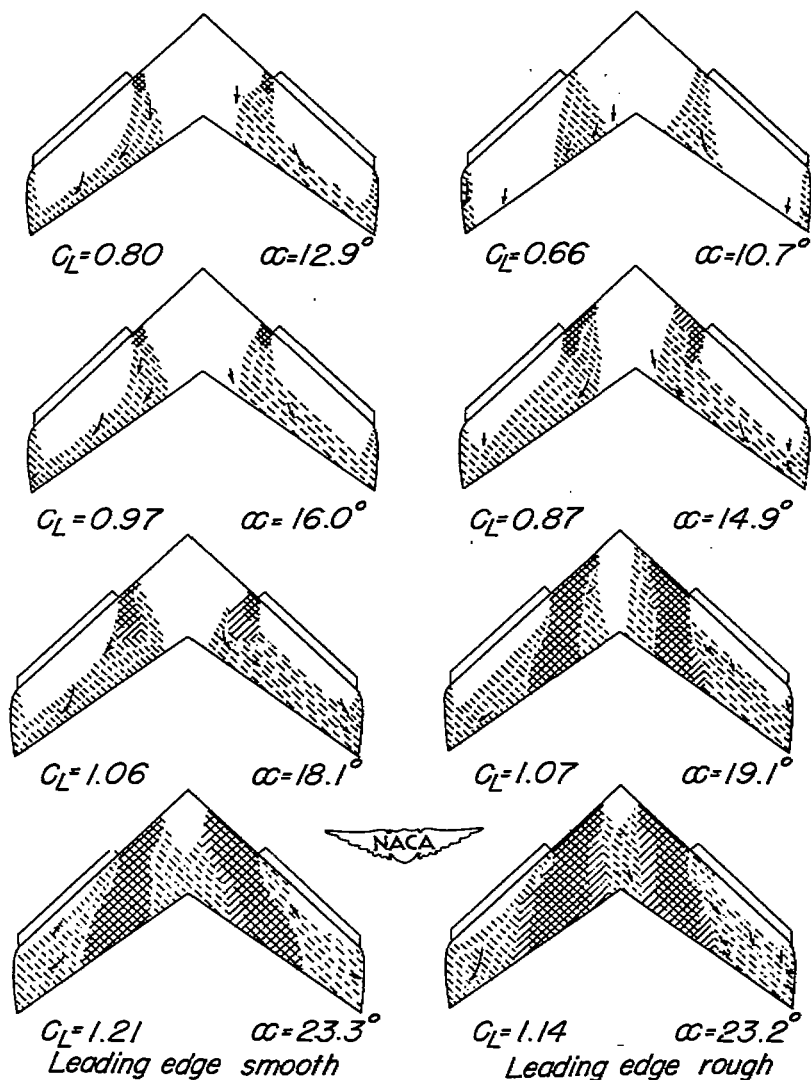
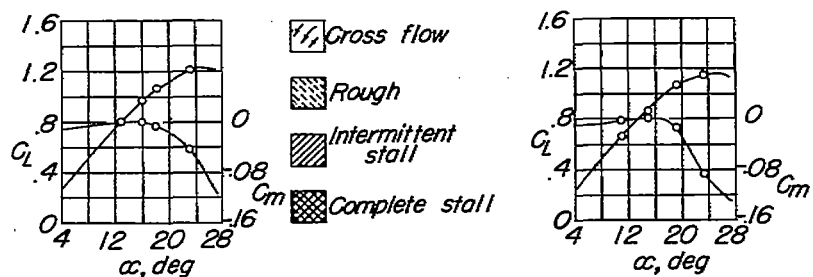
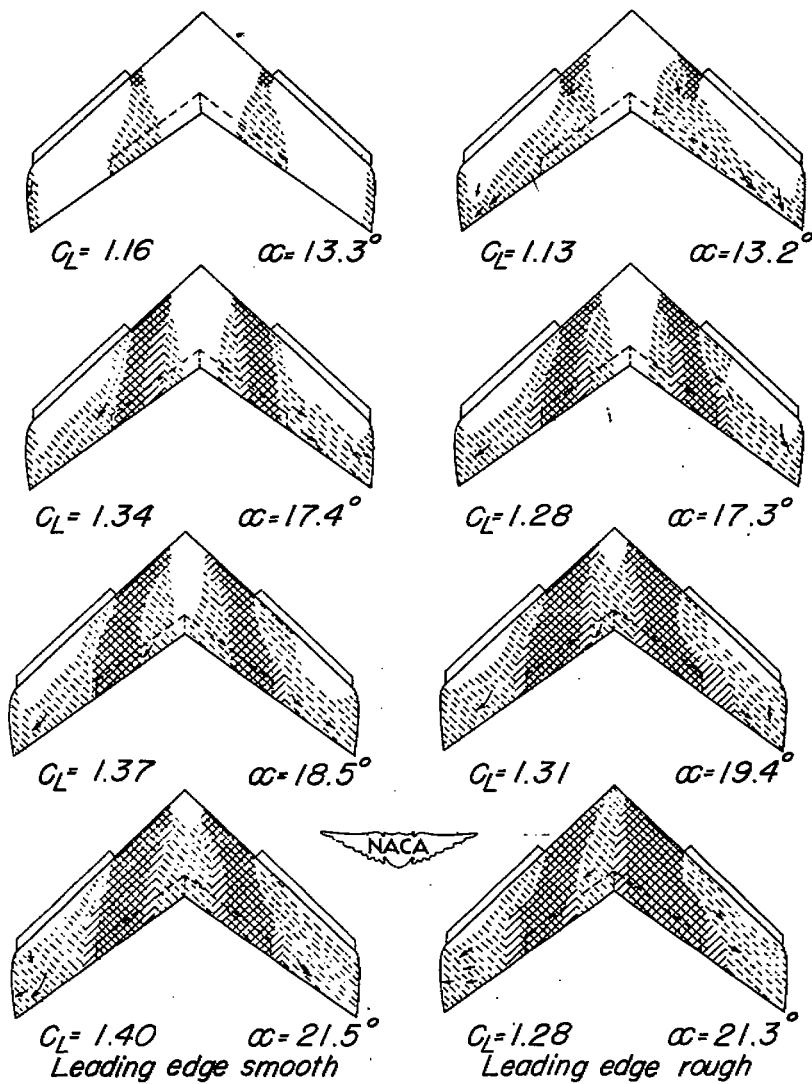
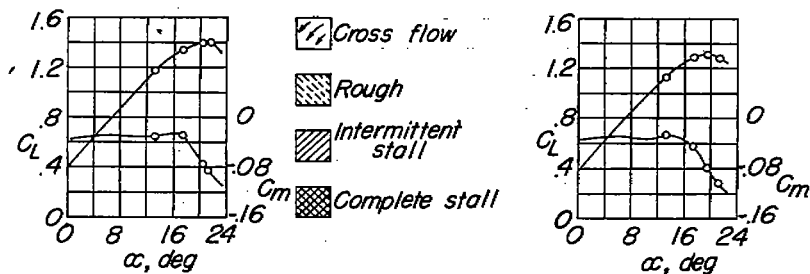


Figure 12.- Effect of roughness on the stalling characteristics of the  $42^\circ$  sweptback wing with  $0.725\frac{b}{2}$  leading-edge flaps and half-span split flaps.  $\delta_f = 60^\circ$ ;  $R = 3.0 \times 10^6$ .



(a) Split flaps off;  $R = 4.7 \times 10^6$ .

Figure 13.- Effect of roughness on the stalling characteristics of the  $42^\circ$  sweptback wing with  $0.575\frac{b}{2}$  leading-edge flaps with and without half-span split flaps.  $\delta_P = 60^\circ$ .



(b) Split flaps on;  $R = 3.0 \times 10^6$ .

Figure 13.- Concluded.

NASA Technical Library



3 1176 01436 7370